Automatic Control and Computer Sciences
Vol.35, No.3, pp.11-19, 2001

Avtomatika i Vychislitel'naya Tekhnika
Vol.35, No.3, pp.14-24, 2001

WAVELET DECOMPOSITION AND FRACTAL ANALYSIS FOR JOINT MEASUREMENTS OF LASER SIGNAL DELAY AND AMPLITUDE

A.S. RYBAKOV, *engineer*
Institute of Electronics and Computer Science, Latvian University
Dzerbenes 14, LV-1006 Riga (Latvia)
E-mail: alexryb_lv@mail.ru

A regression algorithm is considered for balancing out the effects of echo signal amplitude spread on the error in range measurement to artificial satellites. Noise excursions can be filtered out in nonstationary sequences of lidar measurements by means of a procedure for multiple-scale wavelet decomposition. The stationarity indicator for the multiple-scale components is provided by the fractal dimensions.

1. INTRODUCTION

When one develops algorithms (brainware) for lidar systems, the software writer naturally wishes to use nontraditional signal processing methods on the latest fast computers. In particular, he may attempt to use algorithms for tasks that until recently were performed either by hardware or by analog means. They include a task traditional for lidar of precision timing for amplitude-fluctuating signals [1].

The range measurement in pulse lidar amounts to measuring the delay of the reflected or stop echo pulse with respect to the radiated or start one. The reflected-signal detector is often a photomultiplier. Its output pulses fluctuate in amplitude on account of the random parameters of the light pulses reflected from the satellite and passing through the atmosphere and also because of the randomness in the light-field transformation and photoelectron multiplication.

Figure 1 shows histograms for the signal amplitudes at the photocell output in the stop channel, which indicate that the reflected signal from the satellite has an amplitude spread considerably wider than that for the signal reflected from an immobile calibration target.

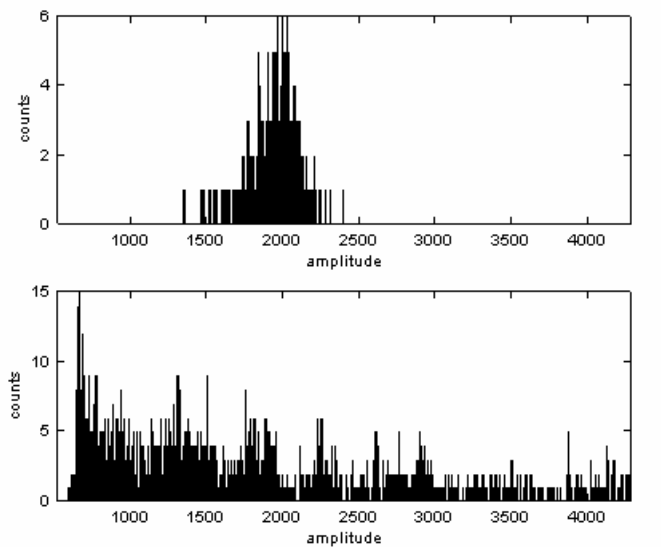

Fig. 1. Reflected-signal amplitude distributions at photocell output in locating a fixed target (upper graph) or a reflector on a satellite (lower graph).

When the signals are timed by a threshold device, the amplitude spread leads to a specific timing error (amplitude-dependent time walk). To balance out the effects from amplitude fluctuations, one usually employs tracking-threshold timers, or constant-fraction discriminators [1, 2], which are complicated analog devices, but at the same time cannot compensate for wide-range amplitude fluctuations.

It is possible to balance out the effects from the echo amplitude spread [3] if in parallel with the measurement of the delay one measures the amplitude of the photocell output. If one can correlate the delay with the amplitude, one can correct the range estimate by means of software.

Nontraditional mathematical methods of compensating for the amplitude spread in lidar ranging by software means include discrete wavelet transformation [4] and fractal dimension analysis [5]. These methods can quite simply produce an algorithm for the regression of the delay on the pulse amplitude that is stable in the presence of noise excursions.

2. REGRESSION OF ECHO SIGNAL AMPLITUDE ON THE DELAY

The general task of regression is to fit a smooth curve to a set of points, with the curve such as to minimize the sum of the squares of the deviations from the observed points. The regression model for simplicity may be taken as nonlinear in the independent variable but linear with respect to the parameters. If the set of points constitutes the set of pairs $\{\tau_i, A_i\}$ from joint delay-amplitude measurements involving a wide range in amplitudes, then the regression curve may serve as a correcting function $\tau(A)$ to balance out the effects of the amplitude spread on the delay estimate.

To generate $\{\tau_i, A_i\}$, one makes parallel measurements on the delay and amplitude for a constant range. To provide the necessary amplitude range in the echo pulses (Fig.1, lower curve), the instrument is applied to an immobile calibration target, for which one periodically varies the transmission of an optical filter over a wide range. The echo amplitudes are converted to time intervals and are measured together with the location delay by the SETIC time interval meter [6].

Figure 2 reflects the correlation between the delay and the amplitude but does not allow one to express it analytically as a single-valued correcting function $\tau(A)$.

The set of pairs $\{\tau_i, A_i\}$ can be represented as a scatter diagram (Fig.3); if the delay and amplitude are correlated, the point set takes the form of a curved noise-corrupted band, while otherwise one gets a dispersed cloud.

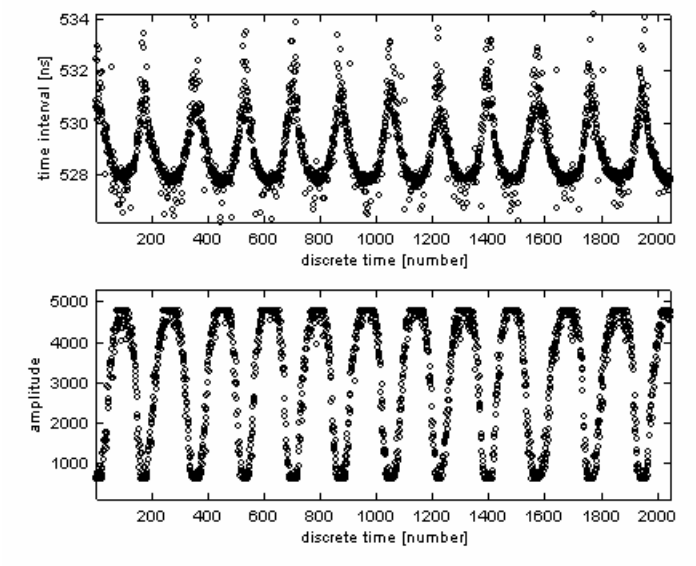

Fig. 2. Sequences of measured delays (top graph) and amplitudes (lower graph) of detector output pulses.

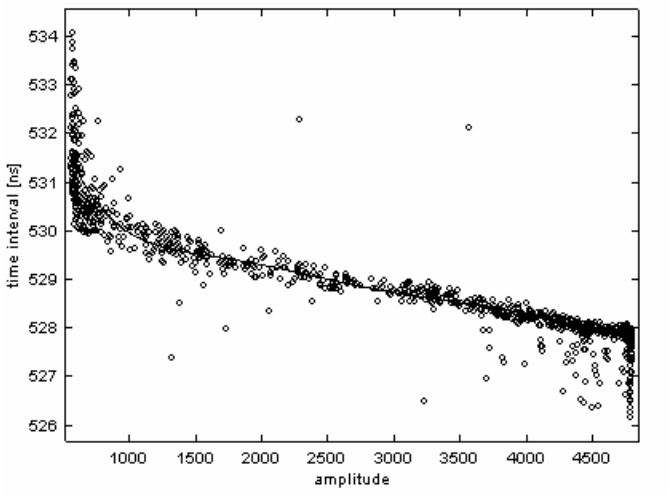

Fig. 3. Scatter diagram for echo delay and amplitude; the solid line is the regression curve.

The regression method is not stable in the presence of noise excursions and works well only when they are absent from the $\{A_i\}$ and $\{\tau_i\}$ sets. The excursions should not be included in the input data for the model, since otherwise one cannot guarantee accuracy in correcting the measurements. The data sequences are realizations of nonstationary processes (Fig.2), so one cannot apply directly a threshold treatment of two-sided limiting at the level of two or three sigma, where sigma is the standard deviation. The excursions are usually concealed within the range of true values for the data, and two-sided threshold treatment would merely truncate the range.

The concept for selecting excursions in a nonstationary sequence is as follows. One isolates a fairly smooth regular nonstationary component in the sequence, which is then subtracted from the data. After this, one can readily exclude anomalous noise excursions on the two-three sigma rule. The $\{A_i\}$ and $\{\tau_i\}$ discrete sequences are filtered by multiple-scale decomposition in a certain wavelet basis [7]. The extent to which these various-scale components are nonstationary can be checked from their fractal dimensions.

3. FORMULAS FOR WAVELET DECOMPOSITION AND FRACTAL ANALYSIS

Multiple-scale or multiresolution analysis represents an algorithmic realization of the discrete wavelet transformation, which is based on subband coding [8, 9].

The following are formulas for decomposing a signal at level j, $S_j[n]$, into a smoothed part $S_{j+1}[n]$ and details in the form of wavelet coefficients $W_{j+1}[n]$ [7]:

$$S_{j+1}[n] = \sum_{k=0}^{L-1} h[k]\, S_j[(2n+k) \bmod (N/2^j)]\,, \tag{1}$$

$$W_{j+1}[n] = \sum_{k=0}^{L-1} (-1)^k h[L-1-k] S_j[(2n+k) \bmod (N/2^j)]\,, \tag{2}$$

in which

$$n = \overline{0, N/2^{j+1} - 1}\,, \tag{3}$$

in which N is the number of samples on the initial signal, j = 0, 1, 2,... are the numbers of the scale levels, $h[k]$ are the coefficients in the low-frequency scaling filter, which generates the corresponding wavelet basis, and L is the number of filter coefficients. The initial signal is associated with a component $S_0[n]$ at zero level (j = 0).

The formula for reconstructing the signal at level j, $S_j[n]$, from the components $S_{j+1}[n]$ and $W_{j+1}[n]$ at the decision level j + 1 is as follows [7]:

$$
\begin{aligned}
S_j[n] \;=\; & \sum_{k=0}^{L/2-1} h[L-1-2k-(n+1) \bmod 2] \times \\
& \times S_{j+1}\left[\left(\frac{N}{2^{j+1}}-\frac{L}{2}+1+k+\operatorname{int}\left(\frac{n}{2}\right)\right) \bmod \left(\frac{N}{2^{j+1}}\right)\right] + \\
& + (-1)^n \sum_{k=0}^{L/2-1} h[2k+(n+1) \bmod 2] \times \\
& \times W_{j+1}\left[\left(\frac{N}{2^{j+1}}-\frac{L}{2}+1+k+\operatorname{int}\left(\frac{n}{2}\right)\right) \bmod \left(\frac{N}{2^{j+1}}\right)\right],
\end{aligned}
\tag{4}
$$

in which

$$
n = \overline{0, N/2^j - 1}, \tag{5}
$$

in which int(z) is the integer part of z and $j = 0, 1, 2,....$

Expressions (1) and (2) correspond to direct discrete wavelet transformation, while (4) represents the inverse. It is best to use a filter with a small number of coefficients such as a Daubechies-4 filter with four coefficients:

$$
h[0] = (1/\sqrt{2})(1+\sqrt{3})/4, \tag{6}
$$

$$
h[1] = (1/\sqrt{2})(3+\sqrt{3})/4, \tag{7}
$$

$$
h[2] = (1/\sqrt{2})(3-\sqrt{3})/4, \tag{8}
$$

$$
h[3] = (1/\sqrt{2})(1-\sqrt{3})/4, \tag{9}
$$

or a Haar filter with only two:

$$
h[0] = h[1] = 1/\sqrt{2}. \tag{10}
$$

If one selects the Haar basis, it is convenient to use unnormalized filter coefficients, and then the wavelet expansion can be reduced to the sequential calculation of half-sums and half-differences of the even and odd elements in the sequence:

$$
S_{j+1}[n] = (S_j[2n] + S_j[2n+1])/2, \tag{11}
$$

$$
W_{j+1}[n] = (S_j[2n] - S_j[2n+1])/2, \tag{12}
$$

where n varies in the range defined by (3); the wavelet reconstruction amounts to summation and subtraction:

$$
S_j[n] = S_{j+1}[\operatorname{int}(n/2)] + (-1)^n W_{j+1}[\operatorname{int}(n/2)], \tag{13}
$$

where n varies over the range defined by (5).

Rapid classification of signals at various scale levels as stationary or nonstationary is conveniently based on their fractal dimensions. The fractal dimensions of a compact subset Y in metrical space are [5] given by the limit

$$
D_f = -\lim_{r \to 0} \frac{\ln M(r)}{\ln r}, \tag{14}
$$

in which $M(r)$ is the minimum number of open spheres of radius r necessary to cover subset Y. The sequence of samples from a one-dimensional signal may be considered as a set of points in a plane covered by circles of radius r. The fractal dimensions for a one-dimensional signal are related to the waveform complexity and the stochastic parameters and nonstationary behavior as follows:

$$1 \le D_f \le 2 . \tag{15}$$

Empirical estimation of the fractal dimensions for a discrete sequence $y[n]$ composed of N terms can be provided by the following fairly fast algorithm.

1. We choose the radius of the covering circles:

$$r = \frac{1}{2(N-1)} . \tag{16}$$

2. We calculate the number of covering circles from

$$M(r) = \text{int}\left(\frac{\sum_{n=1}^{N-1} \sqrt{(\tilde{y}[n] - \tilde{y}[n-1])^2 + (2r)^2}}{2r} \right), \tag{17}$$

in which

$$\tilde{y}[n] = (y[n] - y_{\min}) / (y_{\max} - y_{\min}) - \tag{18}$$

is a sequence normalized to the range of the instantaneous values [0..1], while $y_{\min}$ and $y_{\max}$ are the minimal and maximal values of the elements in the initial sequence $y[n]$.

3. We compute and store $\ln M(r)$ and $\ln r$ for the given circle radius.

4. The normalized sequence $\tilde{y}[n]$ is halved in length by discarding the even or odd elements (N is halved) and then going to the first point in the algorithm.

After k cycles, we obtain the vectors

$$[\ln M(r_1),\ \ln M(r_2) \ldots \ln M(r_k)]^T \tag{19}$$

and

$$[\ln r_1,\ \ln r_2 \ldots \ln r_k]^T . \tag{20}$$

If we fit a straight line as a regression curve to the data from these vectors, then its slope with the sign reversed gives the fractal dimensions.

The fractal dimensions characterize the waveform complexity and can serve as a classification feature (indicator) in the recognition of stationary and nonstationary sequences.

4. WAVELET FILTRATION IN REGRESSION LINE FITTING

Multiple-scale decomposition in terms of resolution levels involves the sequential performance of forward and reverse wavelet transformations in accordance with (1), (2), and (4), but before we perform the inverse transformation, one sets as zero all the resolution levels apart from the one being analyzed. When one uses unnormalized Haar filters, the wavelet transformation is performed in accordance with the simplified formulas (11)-(13).

That decomposition for a sequence of measured delays (upper curve in Fig.2) in the Haar wavelet basis and Daubechies basis is shown respectively in Figs.4 and 5.

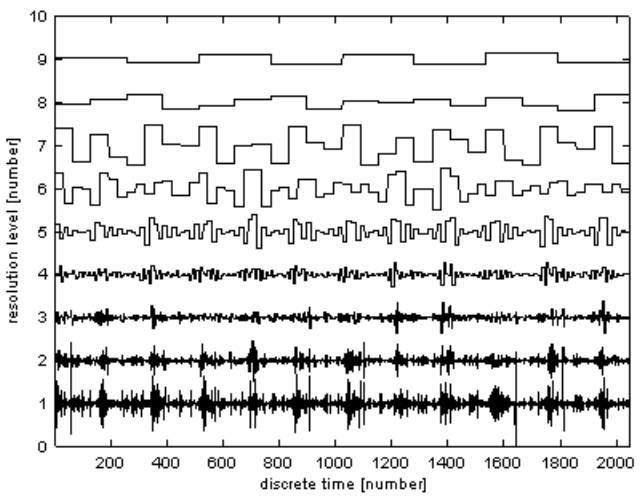

Fig. 4. Multiple-scale decomposition of a sequence of delays in the Haar wavelet basis.

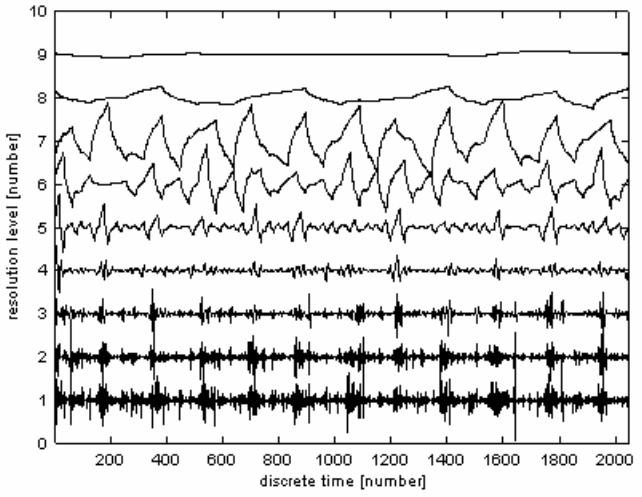

Fig. 5. Multiple-scale decomposition of a delay sequence in the Daubechies-4 wavelet basis.

These diagrams imply that the signal components in small-scale (high-frequency) resolution levels are very similar no matter what the wavelet basis used. The values for the fractal dimensions of the components at three small-scale levels (Fig.6) are close to or exceed D_f = 1.5, which is usually employed as the boundary between stationary and nonstationary random processes. Therefore, it is best to select the simplest Haar wavelet basis. The stationary noise component in the sequence can be reconstructed from the components at two or three small-scale levels.

When the stationary noise component has been reconstructed, the two-sided threshold excursion selection for the given level is applied (lower graph in Fig.7). The excursions are selected in sequence from the set of delays for the set of amplitudes and vice versa. If some element in the set of delays corresponding to instant k in discrete time, such as τ_k , is eliminated in the processing, then one also eliminates element A_k from the set of amplitudes corresponding to instant k.

The data filtered in that way form a set of points (scatter field) for which one constructs the nonlinear regression line.

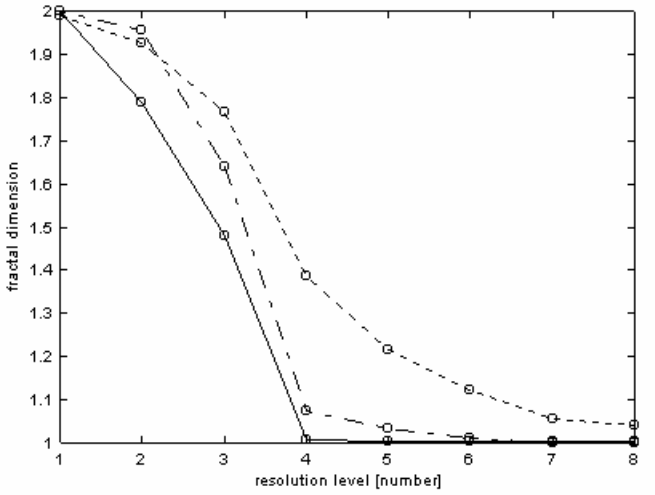

Fig. 6. Fractal dimensions of wavelet components from a discrete signal (top graph in Fig. 2) at various scale levels; for clarity, the discrete values have been joined by the following lines: solid line Haar wavelet basis, dashed line Daubechies-4 wavelet basis, dot-dash line Symmlet-10 wavelet basis.

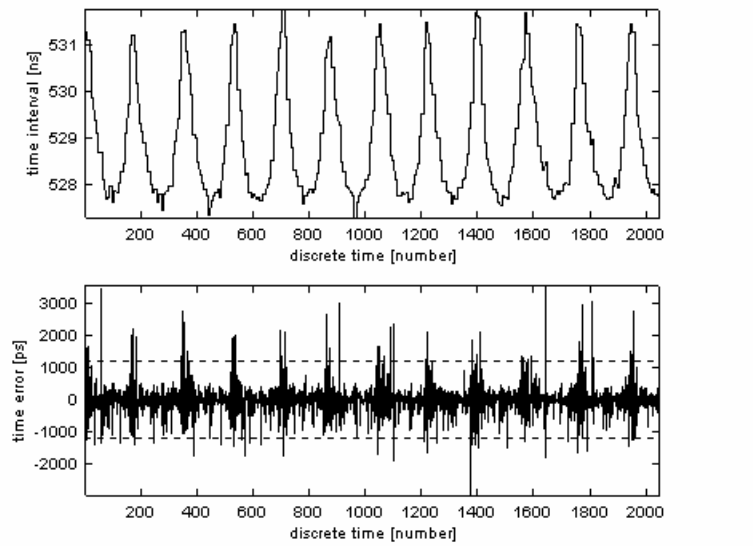

Fig. 7. Regular component (upper graph) and noise component (lower graph) of a delay sequence. The dashed lines show the threshold levels for selecting excursions.

We now quote estimates of fractal dimensions for reconstructed sequences (Fig.7): the regular nonstationary component (upper graph) with $D_f = 1.017$ and the stationary noise component (lower graph) with $D_f = 1.993$.

Figure 8 shows the performance of the algorithm stable against anomalous noise excursions for the correction of the measured delays by reference to the amplitude data, which shows the results for an immobile calibration target used with periodic transparency change in the optical filter.

Wavelet filtration with regression for $\tau(A)$ enables one to correct measurements and thus reduce the standard deviation in measuring the delay by more than a factor 4. For example, the results given in the upper graphs in Figs. 2 and 8 show that the error is reduced from 1350 to 220 picoseconds (sample volume $N = 2400$). For comparison we note that the correcting function obtained by fitting a regression line to the $\{\tau_i , A_i\}$ pair set without selecting the excursions enables one to reduce the error to 450 picosec after correction, i.e., the error is twice as large.

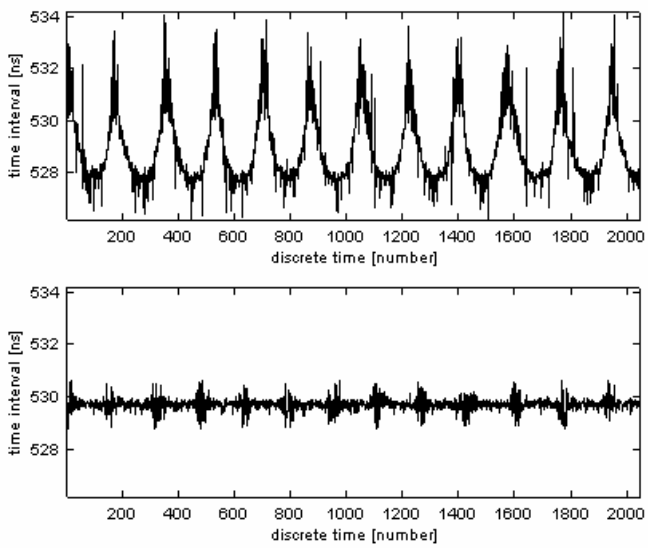

Fig. 8. Results from correcting measured echo delays from an immobile calibration target. Upper graph measured delay sequence before correction, lower graph after correction.

5. CONCLUSIONS

Importance attaches to the methods of freeing nonstationary sequences from noise excursions in the software implementation of an excursion-stable regression algorithm for compensating for the effects of echo signal amplitude spread on the error in estimating the location delay. To select latent anomalous excursions in a nonstationary sequence of lidar measurements, one uses a multiple-scale decomposition in the Haar wavelet basis. The randomness and stationarity indicators for the multiple-scale components are provided by the fractal dimensions.

These processing algorithms have been implemented in my SETICPRO software used with the SETIC lidar system at the RIGA 1884 satellite observation station.

These methods can be applied in processing joint measurements of delay and amplitude for echoes from the GFO-1 satellite, which have provided a standard deviation in the range of 1.77 cm after correction, as against 4.59 cm before it.

REFERENCES

[1] A. B. Sharma, “Receiver design for laser ranging to satellites”, IEEE Trans. on Instrument. and Measurement, vol. IM-30, no. 1, pp. 3-7, 1981.

[2] M. O. Bedwell and T. J. Paulus, “A versatile constant-fraction 100 MHz discriminator”, IEEE Trans. on Nuclear Science, vol. NS-25, no. 1, pp. 86-92, 1978.

[3] A. V. Potapov and A. F. Chernyavskii, *Statistical Measurement Methods in Experimental Nuclear Physics* [in Russian], Atomizdat, Moscow, 1980.

[4] I. Daubechies, Ten Lectures on Wavelets, CBMS-NSF Lecture Notes No. 61, SIAM, Philadelphia, 1992.

[5] B. B. Mandelbrot, Fractals: Form, Chance and Dimension, Freeman, San Francisco, 1977.

[6] Yu. Artyukh, V. Bespal’ko, A. Rybakov, and V. Vedin, “Advanced time interval counter and analyzer based on EET-method application”, Proceedings of the 1999 International Workshop on Sampling Theory and Application, August 11-14, 1999, Loen, Norway, pp. 194-197.

[7] A. S. Rybakov, “Multiple-scale signal analysis in accuracy tests on computer chronographs”, AVT, no. 6, pp. 24-33, 1999.

[8] M. Smith and T. Barnwell, “Exact reconstruction techniques for tree-structured subband coders”, IEEE Trans. on ASSP, vol. ASSP-34, no. 3, pp. 434-441, June 1986.

[9] S. Mallat, "A theory for multiresolution signal decomposition: The wavelet representation", IEEE Trans. on Pattern Analysis and Machine Intelligence, vol. 11, no. 7, pp. 674-693, 1989.

Received 29 September 2000 (originally submitted 11 September 2000)